DISTRIBUTION STATEMENT A. Approved for public release; distribution is unlimited.

Dynamic Simulations of Realistic Upper-Ocean Flow Processes to Support Measurement and Data Analysis

Lian Shen
St. Anthony Falls Laboratory
and Department of Mechanical Engineering
University of Minnesota
Minneapolis, MN 55455
phone: (612) 625-7527 fax: (612) 624-5230 email: shen@umn.edu

Award Number: N00014-14-1-0449

LONG-TERM GOALS

The primary focus of this research is to use computer simulations as a useful research tool to understand the mechanisms of the interactions among Langmuir cells, waves, and currents. This project is intended to be a modeling component of the over Langmuir Cell DRI. Our ultimate goal is to advance our understanding of and establish an efficacious modeling capability for upper ocean boundary layer (OBL) processes to serve for Navy applications.

OBJECTIVES

The scientific and technical objectives of our research in this project include:

- Directly capture the generation and evolution of Langmuir cells in simulations; quantify the statistics of Langmuir turbulence.
- Investigate the onset of wave breaking; quantify wave breaking intensity and model the resultant injection of turbulence to upper ocean; study wave breaking effect on Langmuir cells.
- Develop physics based wind force modeling for oceanic flows; investigate the impact of spatial and temporal variations of wind forcing on waves, currents, and Langmuir cells.
- Investigate effects of surface waves on upper OBL and mixed layer; identify and quantify the key turbulence mixing and transport processes in the flow, and model their dependence on environmental conditions.

APPROACH

Our project builds on a suite of advanced computational tools, including: (i) Wave-surface-fitted LES, which can explicitly resolve phase-resolved wave effect in the simulation of near-surface turbulence and thus has the capability of directly capturing the formation and evolution of Langmuir cells without the rigid-lid approximation used in traditional LES; (ii) Phase-resolved wave simulation, which can compute the nonlinear evolution of wave-field; (iii) Multi-fluids simulation of air-water mixed flow, which can compute wave breaking; and (iv) A novel dynamic sea-surface roughness model, which together with wind LES can yield accurate modeling of wind forcing on upper ocean flows

dynamically according to environmental conditions. Enabled by these sophisticated simulation tools, we will match the realistic field conditions in the DRI for the direct comparison with field observations.

In this project, we will perform dynamic simulations of upper-ocean flows with many of the constraints in the existing models removed. Specifically, we aim to perform simulations for realistic wind and waves conditions, with the interactions of currents and turbulence with dynamically evolving waves directly captured. As a result, the formation and evolution of Langmuir cells, the injection of momentum and energy from wave breaking to the ocean, the forcing by wind, and the processes of turbulence production, transport, and dissipation in the upper OBL and mixed layer can be elucidated and quantified in a physics-based computational framework for the first time. Such computations will be carried out in close collaboration with the field measurement in the DRI. We will use our simulations as a useful tool to help the validation, assimilation, synthesis, and interpretation of measurement data.

WORK COMPLETED

Our research in FY15 focused on performing wave-surface-fitted simulations with wind-driven shear at the wavy surface to capture Langmuir cells directly. We have also adapted our LES code for simulations using the traditional method based on the Craik-Leibovich model, which includes a vortex force in a rigid-lid domain. We also continued the analysis of Reynolds shear stress beneath surface waves, which is important for modeling the wave-turbulence interaction process in the upper ocean.

RESULTS

1. Using our wave-surface-fitted code to capture Langmuir cells directly.

   Wave-surface-fitted simulations have been performed to investigate the formation and evolution of Langmuir cells. In the simulations, a wind-driven shear stress is specified at the wave surface, and the amplitude of the waves is dynamically maintained. The wave motions are directly resolved in the simulation, so that the effects of instantaneous wave distortion and Stokes drift velocity are both included. Based on the simulation data, we have applied triple decomposition to obtain the wind-driven current, wave motions, and turbulence fluctuations. The wave-surface-fitted simulation has been shown to be capable of capturing Langmuir cells.

   Figure 1 plots the streamwise averaged fluctuating velocity field, which is associated with Langmuir circulations. The turbulent Langmuir number is 0.4. Stratification is not considered here. As shown, a pair of counter-rotating vortices are formed in the domain. The downwelling region is much narrower than the upwelling region, with the downwelling speed larger than the upwelling speed. The distribution of spanwise velocity on the surface also indicates a convergence zone above the downwelling region. The streamwise velocity in the downward region is positive, indicating that particles in this region travels faster in the downwind direction. The features of the circulation structures are typical of Langmuir turbuence, indicating the capability of our wave-resolving simulation of directly capturing Langmuir cells.

2. Using the traditional rigid-lid LES with vortex force to simulate Langmuir turbulence in the upper ocean.

   To investigate the influence of the surface waves on the turbulence, we incorporate the Craik-Leibovich model in our rigid-lid LES, with a vortex force involved. A case of pure shear

turbulence driven by a constant surface shear stress is also simulated for comparison. The Reynolds number based on the surface friction velocity u*, the depth of the water H, and the water viscosity ν is 10^6. For the case using Craik-Leibovich model, the turbulent Langmuir number La_t, which is the square root of the ratio of surface friction velocity to the wave Stokes drift velocity, equals 0.3, and kH equals 10. The computational domain is $2\pi H \times 2\pi H \times H$ in streamwise, spanwise, and vertical directions, respectively, and we use a grid of 256×256×256.

Figure 2 shows the streamwise averaged fluctuating velocity field. The velocity vectors clearly show the existence of Langmuir circulations, revealed by pairs of counter-rotating streamwise vortices. Under the surface convergence zone, the relative high-momentum region of streamwise velocity is accompanied by strong downwelling motions, which can deliver the high-momentum flows near the surface into the lower-momentum region in the deeper water. Beneath the surface divergence zone, the streamwise velocity is much lower, because the upwelling motions of Langmuir circulations transport the low-momentum flows in the deeper water to the surface. This transport process contributes to the mixing of momentum and turbulence kinematic energy.

Figure 3 shows the profiles of the mean streamwise velocity. In the near-surface region, the gradient of the mean velocity in the Langmuir turbulence is much smaller than that in the pure shear turbulence. The more uniform mean velocity profile is related to the strong mixing effect of the Langmuir circulations.

This mixing effect can also be shown by the streamwise Reynolds normal stress in Figure 4. The streamwise normal stress in the Langmuir turbulence almost reaches a constant value except for in the region adjacent to the surface, but in pure shear turbulence this stress obviously varies along the vertical direction. Compared with the pure shear turbulence, the vertical and spanwise Reynolds normal stresses are enhanced in Langmuir turbulence.

3. Analyzing effects of surface waves on Reynolds shear stress in an initially isotropic turbulence without mean shear.

   The Reynolds shear stress is an important quantity in the study of wave-turbulence interaction. It is found that Reynolds shear stress is strongly dependent on the wave phases due to the distortion effects of waves. The analysis on the stress budget terms has shown that the wave production and velocity-pressure-gradient terms together contribute to the variation of Reynolds stress under different wave phases.

   Figure 5 shows the Reynolds shear stress near the surface in the wave-following Eulerian frame. Turbulence shear stress is positive under the backward slope and negative under the forward slope. The maximum and minimum of shear stress occur under the backward slope and the forward slope, respectively. Figure 6 shows the generation of shear stress due to the wave strain rate. The production term, $-\langle u'^2 \rangle \partial \langle w \rangle / \partial x$, is negative under the wave crest and positive under the wave trough. The term $-\langle w'^2 \rangle \partial \langle u \rangle / \partial z$ decreases towards the surface due to the blocking effect, and is much smaller than the other production term. Figure 7 shows the velocity-pressure-gradient terms, which are associated with the pressure fluctuation. The term $-\langle w' \partial p' / \partial x \rangle$ is positive under the surface. The second term, $-\langle u' \partial p' / \partial z \rangle$, is positive under the wave crest and negative under the wave trough. The magnitude of both terms decreases as the depth increases. Comparing the contributions of wave production and pressure terms, we found that the variation of the shear stress is mainly determined by the pressure terms, whereas the production terms offset the effects of pressure. As a result, the shear stress reaches maximum under the backward slope and minimum under the forward slope.

IMPACT/APPLICATIONS

Many of our simulation results are the first of their kinds. Using LES tools at different levels of sophistication ranging from our wave-surface-fitted LES, a new wave-directly-forced LES on regular grid, and conventional LES with vortex force and rigid-lid approximation, our goal is to directly test the Craik-Leibovich theory and seek extension and reformulation of existing theories by considering heterogeneity factors such as wave breaking and wave groupness. Together with experimentalists in the DRI, we aim to advance our understanding and modeling capability of Langmuir cells, waves, currents, and upper OBL processes that can serve for Navy applications.

TRANSITIONS

The numerical datasets obtained from this project will provide useful information on physical quantities difficult to measure, and will provide guidance, cross-calibrations, and validations for experiments. As the ultimate application, through the research in this project we will develop an advanced computation framework for the modeling, analysis, and prediction of the upper-ocean interacting processes of Langmuir cells, waves, currents.

RELATED PROJECTS

This project will be performed in collaboration with other investigators in the Langmuir Cell DRI.

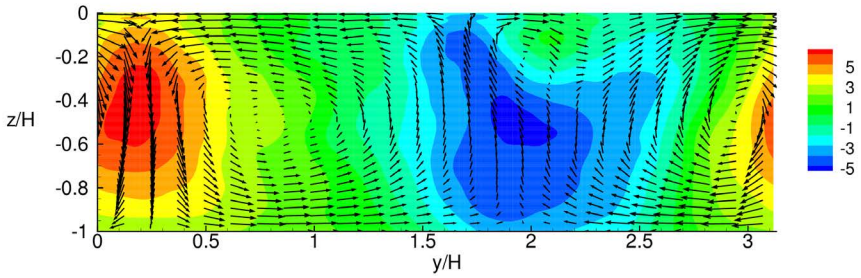

Figure 1. Contours of streamwise averaged fluctuating velocity from the wave-surface-fitted simulation. The vectors denote averaged spanwise and vertical fluctuation velocities.

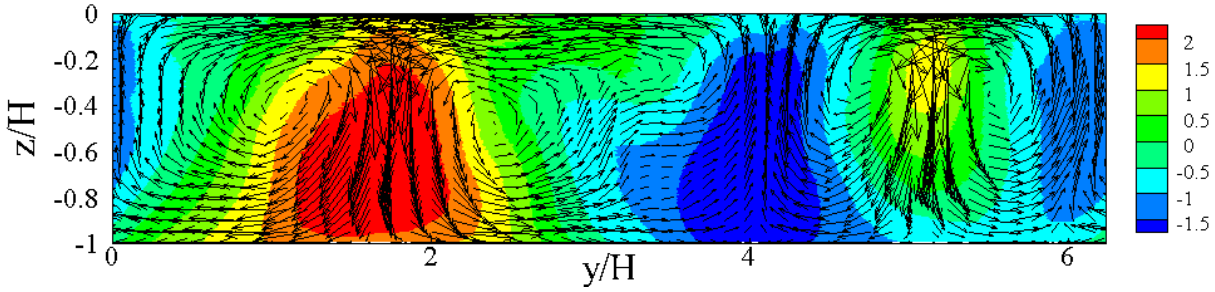

Figure 2. Contours of streamwise averaged fluctuating velocity from the traditional rigid-lid LES using the Craik-Leibovich model. The vectors denote the averaged spanwise and vertical fluctuation velocities.

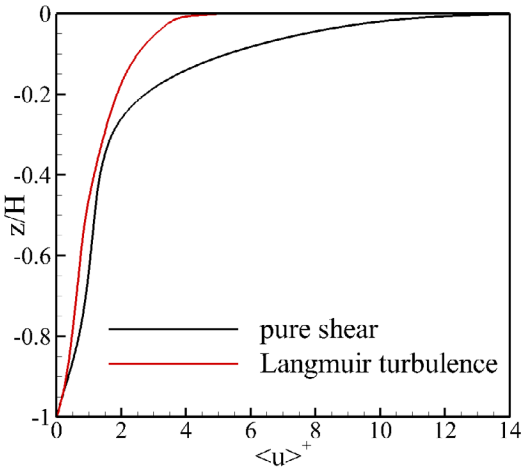

Figure 3. Profiles of the normalized mean streamwise velocity from the traditional rigid-lid LES using the Craik-Leibovich model and comparison with the pure shear case.

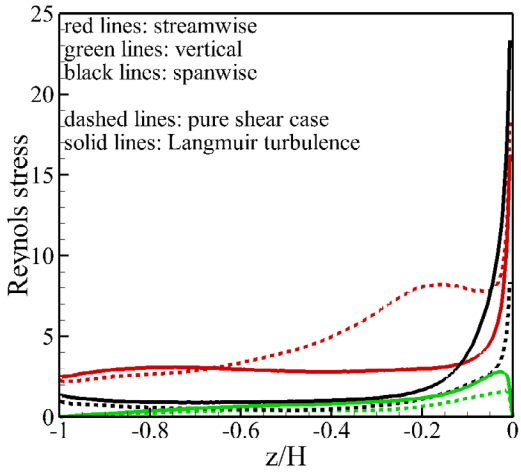

Figure 4. Profiles of the normalized Reynolds normal stresses from the traditional rigid-lid LES using the Craik-Leibovich model.

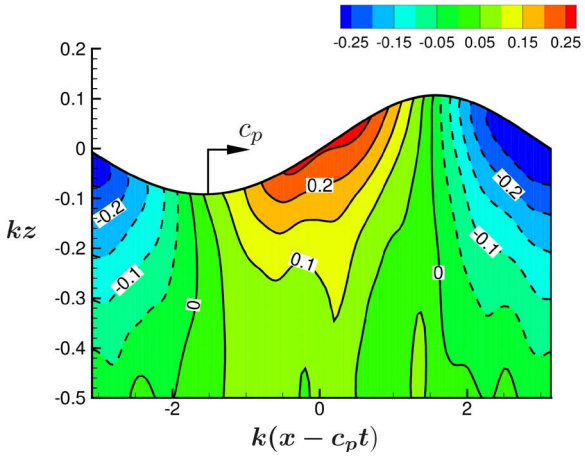

Figure 5. Contours of the normalized turbulence shear stress in the wave-following Eulerian frame. The arrows at the wave crest denote the wave propagation direction.

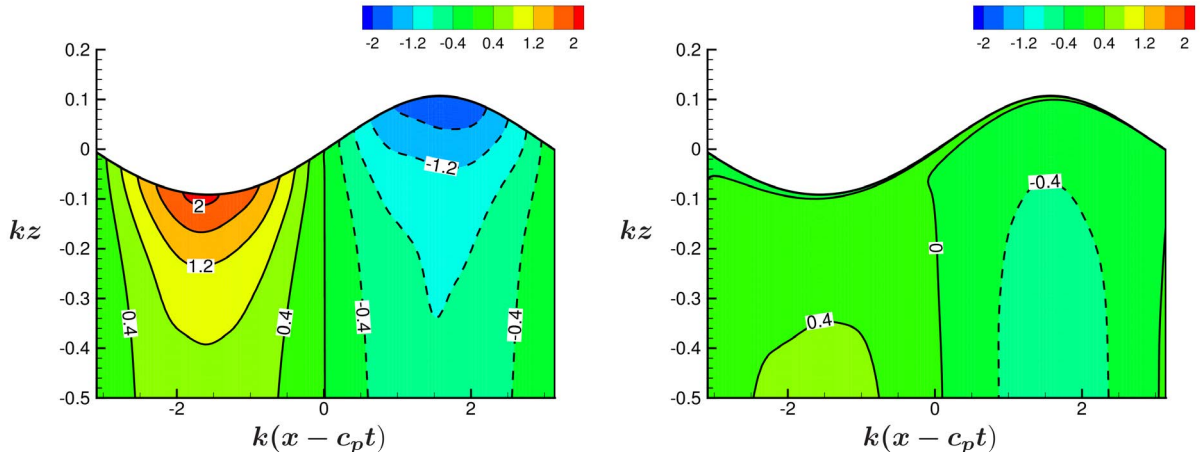

Figure 6. Contours of normalized wave production $-\langle u'^2\rangle \partial\langle w\rangle/\partial x$ (left) and $-\langle w'^2\rangle \partial\langle u\rangle/\partial z$ (right) in the wave-following Eulerian frame.

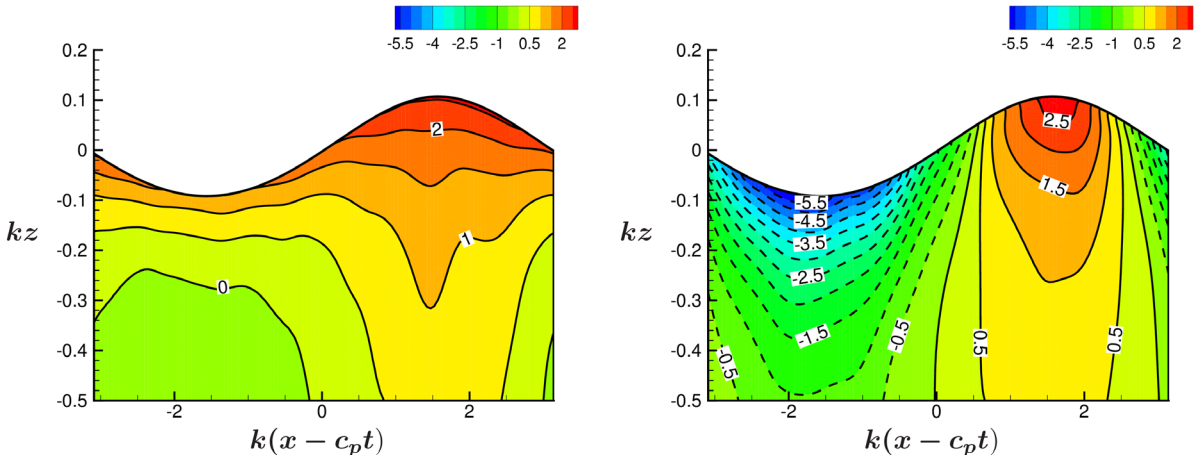

Figure 7. Contours of normalized velocity-pressure-gradient terms, $-\langle w'\partial p'/\partial x\rangle$ (left) and $-\langle u'\partial p'/\partial z\rangle$, in the wave-following Eulerian frame.